

Experimental and theoretical evaluation of surface plasmon-coupled emission for sensitive fluorescence detection

Michal Trnavsky

Dublin City University
Biomedical Diagnostics Institute (BDI)
National Centre for Sensor Research
School of Physical Sciences
Glasnevin
Dublin 9, Ireland

Joerg Enderlein

Eberhard Karls University Tübingen
Institute for Physical and Theoretical Chemistry
Auf der Morgenstelle 8
D-72076 Tübingen, Germany

Thomas Ruckstuhl

University of Zürich
Institute of Physical Chemistry
Winterthurerstrasse 190
8057 Zürich, Switzerland

Colette McDonagh Brian D. MacCraith

Dublin City University
Biomedical Diagnostics Institute (BDI)
National Centre for Sensor Research
School of Physical Sciences
Glasnevin
Dublin 9, Ireland

Abstract. Surface plasmon-coupled emission (SPCE) is a phenomenon whereby the light emitted from a fluorescent molecule can couple into the surface plasmon of an adjacent metal layer, resulting in highly directional emission in the region of the surface plasmon resonance (SPR) angle. In addition to high directionality of emission, SPCE has the added advantage of surface selectivity in that the coupling diminishes with increasing distance from the surface. This effect can be exploited in bioassays whereby a fluorescing background from the sample can be suppressed. We have investigated, both theoretically and experimentally, the SPCE effect for a Cy5-spacer-Ag layer system. Both the angular dependence of emission and the dependence of SPCE emission intensity on Cy5-metal separation were investigated. It is demonstrated that SPCE leads to lower total fluorescence signal than that obtained in the absence of a metal layer. This is the first experimental verification of the reduction in SPCE intensity compared to the metal-free case. Our results are in a good agreement with theoretical models. The validation of the theoretical model provides a basis for optimizing biosensor platform performance, particularly in the context of the advantages offered by SPCE of highly directional emission and surface selectivity. © 2008 Society of Photo-Optical Instrumentation Engineers. [DOI: 10.1117/1.2978067]

Keywords: surface plasmon-coupled emission (SPCE); supercritical angle fluorescence (SAF); fluorescence intensity.

Paper 08050R received Feb. 7, 2008; revised manuscript received May 9, 2008; accepted for publication May 9, 2008; published online Oct. 9, 2008.

1 Introduction

In recent years, there has been an increasing emphasis on the need for highly sensitive detection methods for biomedical applications such as DNA analysis and affinity-based bioassays. In particular, fluorescence-based detection, using fluorescently labeled biomolecules, has been established as the method of choice for detecting low concentrations of analyte. However, there is constant demand for increased sensitivity in order to enable the detection of even lower analyte concentrations. An additional requirement for many assays is the efficient discrimination of analyte emission from background fluorescence in the solution. Techniques such as total internal reflection fluorescence (TIRF) excitation,^{1,2} supercritical angle fluorescence (SAF),³⁻⁵ and surface plasmon-enhanced fluorescence spectroscopy (SPFS)⁶⁻⁸ have been used in the past to achieve surface discrimination. Similarly, surface plasmon-coupled emission (SPCE) may be used for this purpose, as well as providing other advantages.⁹⁻¹⁴

SPCE involves the near-field interactions of excited state fluorophores with a semitransparent thin metal film deposited on a transparent substrate. These interactions result in the generation of surface plasmons that radiate into the substrate. This plasmon-coupled emission is highly directional, and molecules that fluoresce at different wavelengths will emit SPCE at different angles, hence facilitating spectral separation in multianalyte bioassays. Since only the emission from those molecules that are close to the metal surface will couple into the surface plasmon, the technique allows discrimination between molecules that are bound to the surface and those in the bulk sample. The highly directional nature of the emission also facilitates enhanced fluorescence collection efficiency.

SPCE has been investigated experimentally by many authors.⁹⁻¹⁴ There have been some reports of the use of SPCE in bioassays,^{11,15} and SPCE has been used to achieve single molecule detection.¹⁶ Theoretical models have also been developed¹⁷⁻¹⁹ to predict various SPCE properties and account for a range of effects related to the interaction of excited molecules with planar metallic structures. A theoretical study by Enderlein and Ruckstuhl¹⁹ concluded that SPCE does not produce any increase in intensity compared to that detected in

Address all correspondence to: Brian MacCraith, Dublin City Univ., School of Physical Sciences, Biomedical Diagnostics Institute (BDI), National Centre for Sensor Research, Glasnevin, Dublin 9, Ireland; Tel: 00353-1-700-5299; E-mail brian.maccraith@dcu.ie.

the absence of the metal film. In fact, the model predicts that the presence of the metal film leads to a reduction in the detected fluorescence intensity.

The SPCE study reported here employs the commonly used biological label, Cy5, which is separated from a thin silver film by SiO₂ spacer layers of varying thickness. The angular distribution of the SPCE intensity was investigated as a function of spacer layer thickness. The total SPCE intensity was also measured and compared to that measured in the absence of the metal layer. A theoretical analysis of the system was carried out, and the predictions were compared with experimental results.

There is good agreement between the model predictions and the experimentally determined angular distribution of SPCE fluorescence as well as the optimum spacer thickness for maximum integrated SPCE intensity. An overall reduction in detected SPCE intensity compared to that measured in the absence of metal was observed, which is consistent with a recently published theoretical investigation.¹⁹ The key significance of this study is that it is the first experimental verification of the attenuation in SPCE intensity compared to that detected in the absence of the metal layer that was predicted by Enderlein and Ruckstuhl.¹⁹ The close agreement between the model and experimental results provides a basis for optimization of the design parameters for exploitation of the SPCE technique on biochip platforms.

2 Materials and Methods

2.1 Sample Preparation

Chemically cleaned glass microscope slides (Menzel) were used as substrates throughout. To promote the adhesion of the metallic films to the glass substrates, we used the method described in Ref. 20.

Silver (>99.99% purity, Aldrich) was deposited by vacuum deposition in an Edwards Auto 360 vacuum deposition system equipped with e-beam heating apparatus. Deposition of the silver film was followed by growth of the spacer layer (silicon dioxide-fused silica, 99.99%, Aldrich). The growth of the film was monitored *in situ* by a thin film monitor (TFM 5, Edwards). Prior to the dye immobilization step, slides were characterized by measuring the thickness of silver films and determination of thickness/refractive index of the silica films. The measurements were carried out on a spectroscopic ellipsometer (Jobin-Yvon Horiba UVISSEL). The thickness of silver films was determined to be 49 ± 3 nm, and the silica films were deposited with thicknesses ranging from 10 nm to 480 nm. The refractive index of the silica films, as measured at $\lambda = 670$ nm, was found to be 1.46 ± 0.02 , which is very close to the reference value used in the modeling software.

Cy5 fluorescent dye from Amersham Bioscience was immobilized on the silica film. For formation of the dye monolayer, the method of dye modification as described in Ref. 21 was used to facilitate attachment of Cy5 onto the substrate. Dye molecules were conjugated to polyallylamine hydrochloride (PAH), which is a polyelectrolyte with a positively charged termination group. In the immobilization procedure, the slides were first treated in an oxygen plasma chamber (Harrick) for 2 min to establish a high density of negative surface charge. Plasma-treated slides were subsequently im-

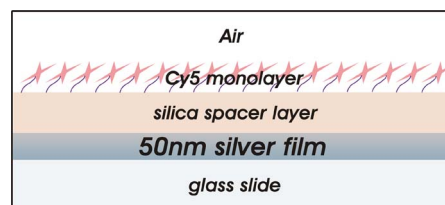


Fig. 1 Schematic of layered film structure for SPCE measurements.

mersed in aqueous solution of Cy5-PAH for 25 min, carefully rinsed in deionized water, and dried. Attachment is achieved by electrostatic attraction of polyelectrolyte/dye molecules to a charged surface. The electrostatic nature of attachment guarantees formation of a molecular monolayer of PAH-Cy5. The cross section of the layered structure is displayed in Fig. 1. For confirmation of the presence of dye on top of the silica film, slides were analyzed in a fluorescence array scanner (Afymetrix, GMS 418). This indicated that the coverage was homogenous and uniform but that the coverage density fluctuated from sample to sample. These fluctuations did not affect the SPCE measurements, as a ratiometric approach was employed.

2.2 Experimental Configuration for SPCE Measurements

The sample slide is attached to a hemicylindrical prism made of BK7 glass that is designed in a manner to ensure that the illuminated spot on the sample lies at the center of curvature of the slide-prism system. The sample is illuminated with a 635-nm laser diode with linearly polarized output. The illuminated area was a 1.5-mm-diam spot. A fixed angle of incidence of 50 deg with respect to the sample normal was chosen to enable excitation of both vertically and horizontally oriented dipoles. The prism-sample assembly positioned on a motorized rotary stage (Physik Instrumente) co-rotates with the laser diode. A schematic of the excitation-detection system is shown in Fig. 2. For the measurement, only *p*-polarized laser radiation was used (electric field vector lying in the plane of incidence, as illustrated in Fig. 2). It can be seen that the sample is excited externally to the prism and emission is detected through the prism at an angle θ . This corresponds to the reversed-Kretschmann configuration,¹⁰ where the excitation is not coupled to a surface plasmon.

For measurement of the angular distribution of emission (ADE), the laser-prism system is rotated through the appropriate angular range, and the intensity corresponding to each angular position is detected with a photomultiplier tube (PMT; Hamamatsu H6780-20) that is coupled to a photon counting unit (Hamamatsu C6465). Two emission filters (Omega Optical XF3076) are used to suppress scattered and reflected excitation light. The fluorescent spot-detector distance was 15 cm. A 1-mm-wide vertical slit placed in front of the PMT aperture restricts the acceptance angle to less than 0.5 deg. Rotation and scanning parameters, as well as data acquisition, were computer controlled. All experiments were carried out in air. Using this experimental configuration, both the ADE and the total SPCE intensity were measured. The total intensity was compared to that measured for similar samples without a metal layer.

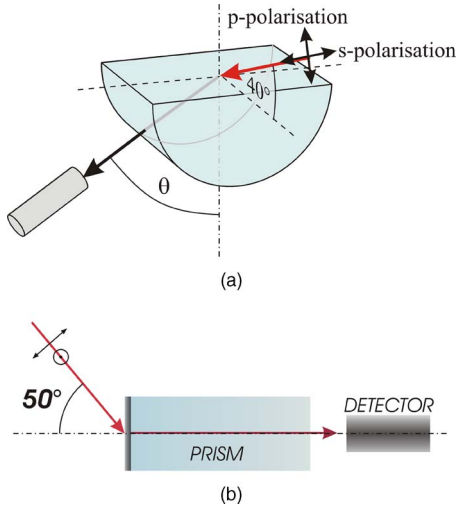


Fig. 2 Experimental geometry used for observation of angular distribution of radiation from fluorophores immobilized on top of a thin silica layer. (a) Perspective view: detector position is fixed, θ represents the actual polar angle of fluorescence emission, and p -polarization of the incident beam denotes that the orientation of the laser electric field is lying in plane of incidence. (b) Experimental geometry—side view: the p -polarized orientation of the laser beam is represented by the arrow lying in the plane of incidence.

3 Theoretical Model

Theoretical calculations of the angular distribution of radiation as well as the detectable emission intensities were performed using a semiclassical electrodynamics approach. Modeling of the excitation and emission properties of fluorescing molecules in layered structures proceeds in several steps. First, the excitation intensity of a molecule of a given orientation and position is calculated. The excitation intensity is proportional (neglecting any saturation effects) to the absolute square of the product of the local electric field amplitude vector and the molecule excitation dipole vector. The electric field amplitude for a planar system can be found in a standard way using Fresnel's reflection and transmission coefficients for plane waves.²² The electric field amplitude of the excitation light is given by

$$\mathbf{E}_{ex} = \sqrt{w_p}[\hat{\mathbf{e}}_p + \hat{\mathbf{e}}'_p r_p(\theta_{inc})] + \sqrt{w_s} \hat{\mathbf{e}}_s [1 + r_s(\theta_{inc})], \quad (1)$$

where $r_{p,s}(\theta_{inc})$ are the reflection coefficients for a plane p - or s -wave incident at angle θ_{inc} on the layered system, w_p and w_s are the relative intensities of the p - and s -wave components of the incident light, $\hat{\mathbf{e}}_p$ and $\hat{\mathbf{e}}'_p$ are unit vectors along the polarization of the incident and reflected p -wave, and $\hat{\mathbf{e}}_s$ is the unit vector along the polarization of the s -wave.

In the second step, the emission of a single molecule with orientation angles (α, β) is considered, where β denotes the inclination toward the vertical axis and α the angle around that axis. The molecule is assumed to be an electric dipole emitter. Then, the electric field amplitude of its emission into direction (θ, ϕ) is given by the general formula

$$\mathbf{E}_{em} = \mathbf{e}_p [A_{\perp} \cos \beta + A_{\parallel}^c \sin \beta \cos(\phi - \alpha)] + \mathbf{e}_s A_{\parallel}^s \sin \beta \sin(\phi - \alpha), \quad (2)$$

where the A_{\perp} , A_{\parallel}^c , and A_{\parallel}^s are functions of emission angle θ but not of α , β , or ϕ . Explicit expressions for A_{\perp} , A_{\parallel}^c , and A_{\parallel}^s can be found in a standard way by expanding the electric field of the dipole emission into a plane wave superposition and tracing each plane wave component through the planar structures using Fresnel's relations.^{19,23,24} It is important to note that the functions A_{\perp} , A_{\parallel}^c , and A_{\parallel}^s depend also on wavelength. As an approximation, we have performed all the calculations for the peak emission wavelength of the fluorophore (670 nm).

Knowing the electric field amplitude of the emission into a given direction (θ, ϕ) , one can then derive the angular distributions of radiation $S(\theta, \phi, \beta, \alpha)$ by

$$S(\theta, \phi, \beta, \alpha) \propto |A_{\perp}(\theta) \cos \beta + A_{\parallel}^c(\theta) \sin \beta \cos(\phi - \alpha)|^2 + |A_{\parallel}^s(\theta)|^2 \sin^2 \beta \sin^2(\phi - \alpha). \quad (3)$$

For calculating the correct emission intensity into a given direction, the right side of Eq. (3) must be normalized to the total emission of the emitter. The total power of emission follows a similar law as the angular distribution of emission in Eq. (3), namely,

$$S_{total}(\beta, \alpha) \propto B_{\perp} \cos^2 \beta + B_{\parallel} \sin^2 \beta, \quad (4)$$

with new weight factors B_{\perp} and B_{\parallel} that take into account also the absorption of emitted energy in the metal layer; for details of their calculation, see Ref. 25.

The measurable angular distribution of radiation is now given by the integral of the product of Eq. (1) (excitation efficiency) and Eq. (3) (emission strength) over all molecule orientations (α, β) weighted with a distribution function of molecule orientations $w(\beta, \alpha)$:

$$I_{em}(\theta, \phi) = \int_0^{\pi} d\beta \sin \beta \int_0^{2\pi} d\alpha w(\beta, \alpha) I_{ex}(\beta, \alpha) \frac{S(\theta, \phi, \beta, \alpha)}{S_{total}(\beta, \alpha)}, \quad (5)$$

where the excitation efficiency $I_{ex}(\beta, \alpha)$ is given by

$$I_{ex}(\beta, \alpha) = |E_{ex,x} \sin \beta \cos \alpha + E_{ex,y} \sin \beta \sin \alpha + E_{ex,z} \cos \beta|^2, \quad (6)$$

with the $E_{ex,x}$, $E_{ex,y}$, and $E_{ex,z}$ being the x , y , and z component of the excitation field amplitude as given by Eq. (1). Although the exact distribution of molecular orientations on the surface is not known, we assumed an isotropic distribution of molecule orientations and set

$$w(\beta, \alpha) = (4\pi)^{-1}. \quad (7)$$

For the model calculations, we used the following values of refractive indices: refractive index of glass $n_{glass}=1.52$; refractive index of SiO_2 $n_{sio}=1.46$; and refractive index of air $n_{air}=1.0$.

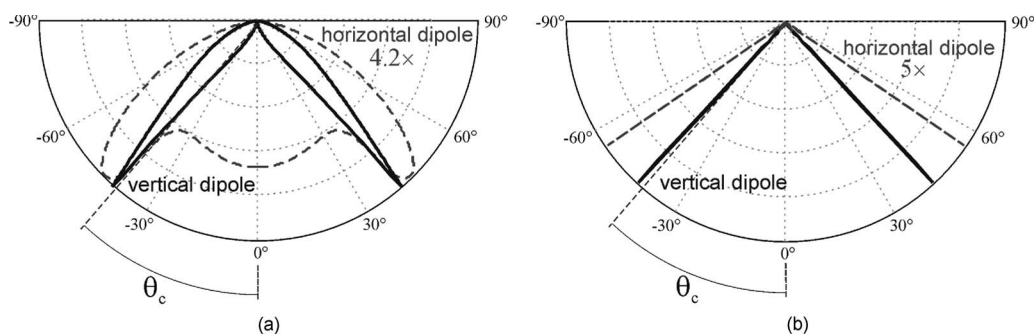


Fig. 3 Model curves of far-field intensity profiles. Fluorescence emerging (a) from dipole emitters placed on the air/glass interface (SAF) and (b) from molecules on top of a 300-nm-thick SiO₂ layer, deposited onto a 50-nm-thin silver film and glass substrate system (SPCE). The (blue line) represents the contribution of purely vertical dipoles (oriented perpendicular to layers), while the (red line) represents the contribution from purely horizontally oriented dipoles (parallel to layers). 4.2× and 5× denotes that the peak emission intensity from the horizontal dipoles is 4.2 times and 5 times, respectively, weaker than from the vertical dipoles with equal strength. The critical angle of total internal reflection of the air/glass interface, denoted as θ_c , is 41.3 deg. (Color online only.)

To allow for inaccuracies in the determination of spacer thickness, this parameter was allowed to vary during fitting. The results of the fitting and comparison with the experiment are discussed in Sec. 4.

4 Results and Discussion

4.1 Angular Distribution of Emission (ADE)

It has been established both theoretically and experimentally^{23,26} that excited fluorescent molecules, which are in close proximity to the interface between two dielectric media, emit a large proportion of their radiation into the environment with higher index of refraction (substrate). The emission pattern is highly anisotropic, with a substantial amount of fluorescence being emitted above the critical angle as a supercritical angle fluorescence (SAF). As SAF is a result of near-field interaction, it allows discrimination between surface and bulk fluorescence and hence is a useful technique for application to biosensors.³ SAF also depends on the orientation of the dipoles of the fluorescent molecules. Figure 3 shows predicted emission curves for (a) SAF and (b) SPCE for the system under investigation. Clearly, a large proportion of the emission occurs above the critical angle 41.3 deg for the system in case (a). The model for prediction of SPCE introduces a 50-nm-thin silver film on the glass and an SiO₂ spacer layer on which the monolayer of dye is located. The emission is now restricted to a narrow angular range that corresponds to angles that satisfy the condition for coupling into the plasmon modes of the metal.

Silver was chosen as the metal for experimental observation of SPCE due to its plasmon resonance in the visible spectrum, which is narrower and more intense than for gold. A thickness of ~50 nm was found to yield the optimum plasmon-coupled fluorescence intensity.^{19,27} Since the dye molecules are concentrated on the surface in the form of a molecular monolayer, this strictly surface-bound immobilization scheme features zero bulk-generated fluorescence and enables both far-field measurement of the fluorophore-layer structure interaction and the observation of fluorescence intensity variations.

Figure 4 shows the experimental and theoretical SPCE emission profiles for the system for a range of different spacer

layer thicknesses. The experimental data are represented by the red dots, while the solid blue lines represent the model data. As expected, fluorescence is emitted into the glass prism in the form of sharp peaks, and the emission occurs only above the critical angle of 41.3 deg. It can be seen from the figure that the angular positions of the peaks increase as the spacer layer thickness increases. At large values of SiO₂ thickness, second and even higher order peaks emerge in both the experimental and theoretical data. The evolution of the emission peak position can be explained as follows: it is well known that minimum reflectivity corresponding to the surface plasmon resonance (SPR) is strongly dependent on even microscopic changes of the local dielectric properties, resulting in an angular shift of the reflectivity curve. Since SPCE is a complementary effect to SPR, the increasing thickness of the spacer is accompanied by an increase in the effective dielectric constant of the system, thus altering the condition for outcoupling of the light via the surface plasmon. In other words, the allowed directions of the fluorescence emission can be attributed solely to the composition of the sample (dielectric properties of the sample at the emission wavelength) and not to the effect of metal-fluorophore separation on the outcoupling mechanism. The varying peak width is related to the plasmon resonance properties of the Ag film.^{18,19} In our case, the peak width varies from 1 deg for a 10-nm spacer layer up to ~5.5 deg for a 120-nm-thick silica layer.

The appearance of multiple peaks for larger metal-fluorophore separations was reported by Gryczynski et al.¹² for a different experimental arrangement and is also in accordance with theoretical predictions.^{18,19} This rising complexity in SPCE peak structure is primarily attributed to the coexistence of surface plasmon modes and waveguide modes within the spacer layer. The number of waveguide modes increases as the spacer layer thickness increases. The existence of the multiple peaks can be explained by competition between the spectrum of allowed coupled-emission modes and the permitted waveguide modes within the spacer layer with metal cladding. Emission of fluorescence at multiple angles is a consequence of the constructive interaction of surface plasmon and waveguide modes.¹⁸ The origin of the extra SPCE peaks was experimentally investigated by measuring their polarization. For small spacer thickness, the single emission peak arises

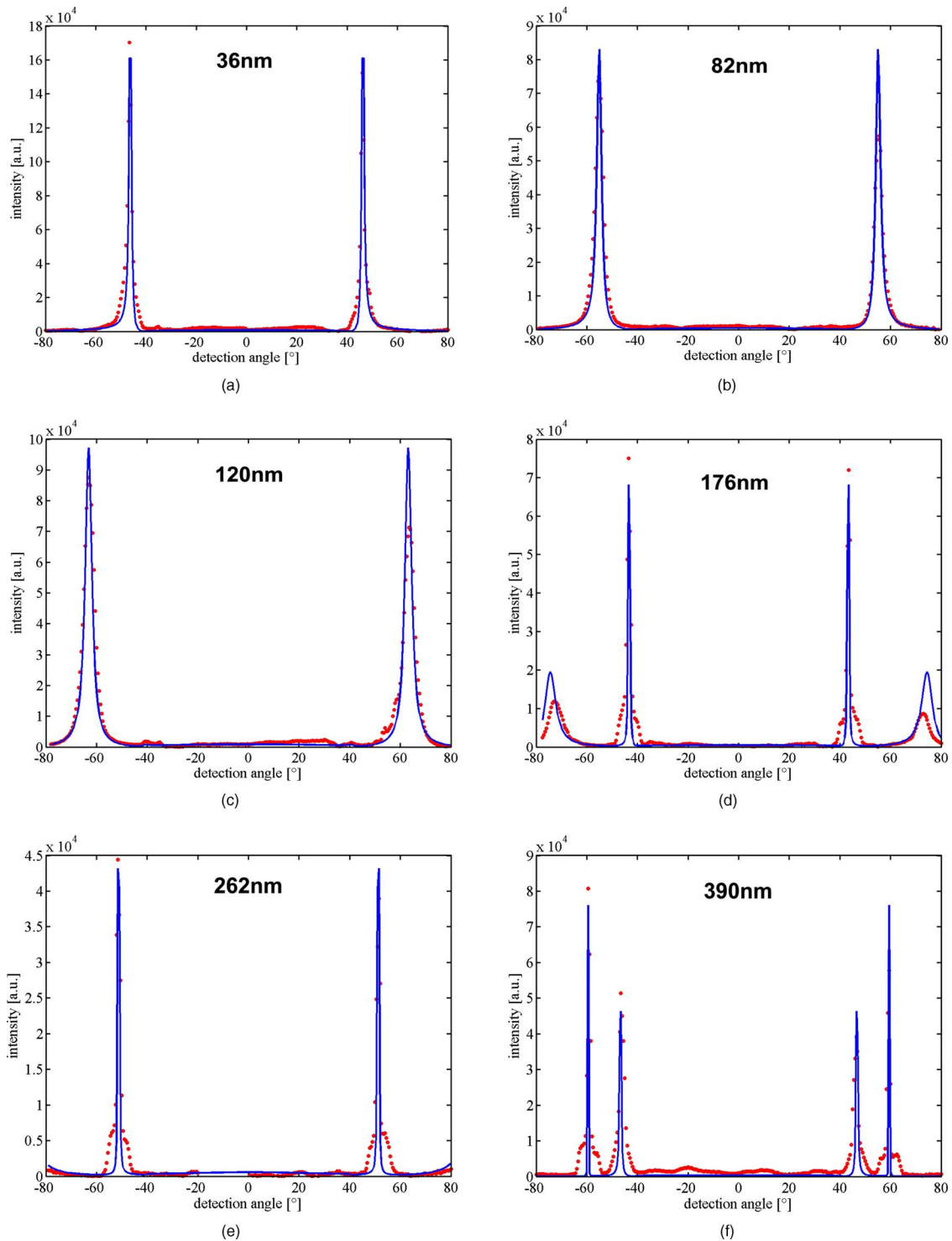


Fig. 4 Experiment-model comparison of SPCE for various values of the spacer thickness. Experimental data (dots) for an experimentally determined spacer thickness are overlaid with best-fit model curves (solid lines).

from coupling of the fluorophore emission to plasmon modes and should therefore be *p*-polarized (polarization axis lying in the detection plane). This was confirmed for the data in Fig. 4, and the results are shown in Table 1. With increasing spacer thickness, the newly emerging peak is *s*-polarized (perpendicular to the detection plane), with every extra higher-angle emission peak having opposite polarization to that of the

lower-angle, purely SPCE peak. The existence of the *s*-polarized peaks supports the theory that the output radiation originates from both plasmon-coupled and waveguide modes.¹⁸

It is clear from Fig. 4 that there is good agreement between the theoretical model and the experimentally measured SPCE emission. The measured emission profiles were initially mod-

Table 1 Experimental results of polarization measurements of the emission peaks for various values of the silica spacer thickness.

Spacer thickness (nm)	Peak position (deg)	Peak polarization
36	47.5	<i>P</i>
120	63.5	<i>p</i>
142	41.5	<i>s</i>
	67.5	<i>p</i>
176	43.5	<i>s</i>
	73.5	<i>p</i>
262	51.5	<i>s</i>
390	46.0	<i>p</i>
	59.0	<i>s</i>

eled using the experimentally determined values of film thickness and refractive index. Isotropic dipole orientation was assumed, and it was taken into account that different dipole orientations are excited with different strength, as described in the previous section. Subsequently, the film thickness was allowed to vary in order to obtain a best fit between theory and experiment for the emission profiles corresponding to different layer thicknesses. In each case, the best-fit thickness value was very close to the experimentally measured value. The graph in Fig. 5 shows the comparison between the experimentally determined spacer thickness values (represented by the solid blue line) and the best fit obtained by the modeling procedure described above (red dots). In the ideal case of perfect experiment-model thickness match, the line and the dots would coincide. The results in Fig. 5 show the good

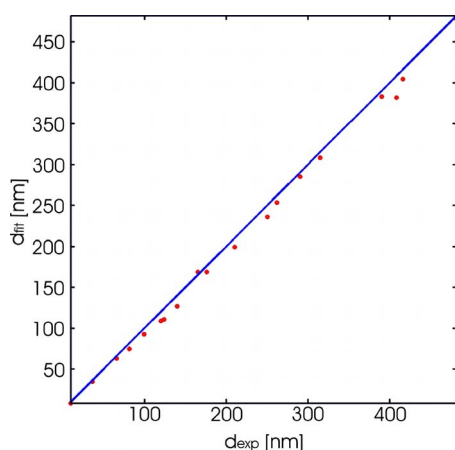


Fig. 5 Comparison between experimentally determined spacer thickness value (solid blue line) and the best fit obtained by the modeling procedure described in the text (red dots). In an *ideal* case of perfect experiment-model match, the dots and the line would overlap. (Color online only.)

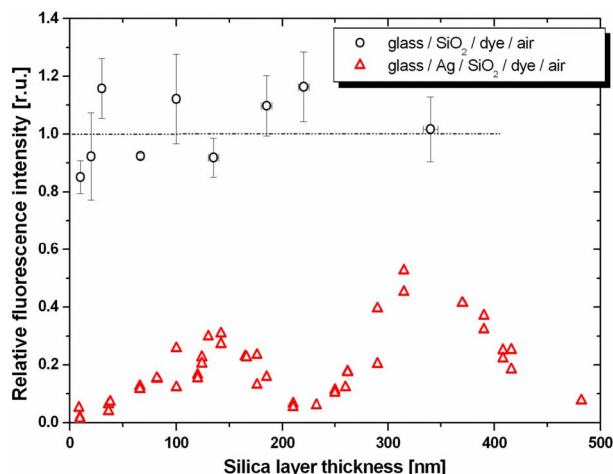


Fig. 6 Effect of semitransparent silver film on fluorescence intensity emitted into the glass slide. Each experimental data point (triangles) represents the ratio of SPCE and non-SPCE intensity for a particular spacer thickness value. For comparison, the metal-free intensity profile is also plotted (circles).

agreement between experimental data and the theoretical model.

The remaining model parameters such as silver film thickness and silver/silica dielectric constants were obtained from ellipsometric measurements ($t_{\text{Silver}}=49$ nm, and $n_{\text{silica}}=1.42$ to 1.46 at 670 nm) and kept constant in the model. The small fluctuations in silver thickness (as reported in the Sec. 2) had a negligible effect on both the shape and width of the peaks. Last, the orientation of the dipoles was modeled, and the best correlation between experimental data and theory was achieved for purely horizontal orientation of molecules (lying in the sample plane).

4.2 Fluorescence Intensity Measurements

A quantitative study was carried out in order to evaluate the SPCE intensity emitted by surface-bound fluorophores into the substrate and to compare it with the intensity in the absence of a metal layer.

Prior to the measurement of the total SPCE intensity, experiments were carried out in order to establish the effect, if any, of the variable-thickness SiO_2 layer on the measured intensity in the absence of a metal layer. Glass slides that were overcoated with silica were prepared for several values of silica thickness, with three to four samples at each thickness, followed by deposition of the Cy5 dye monolayer. The data, which represent multiple scans and include supercritical angle fluorescence, are shown in Fig. 6 (circles). The horizontal line at unity illustrates the ideal case, with zero effect of spacer thickness variations on the intensity. Although the experimental data oscillate about this line, no trend with rising silica thickness is observed, suggesting that the effect of an intermediate SiO_2 layer is negligible. The large error bars are caused by rather large fluctuations of dye surface coverage density from sample to sample.

The situation becomes more complex when the metal film is introduced, because now the emitted intensity depends on

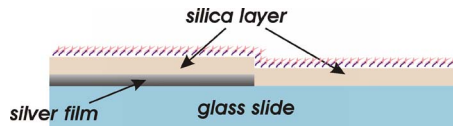


Fig. 7 Cross section of sample used for intensity measurements. Each sample features both metal and metal-free areas, overlaid with silica film with constant thickness. This arrangement allows for direct comparison of the SPCE and non-SPCE intensity.

the distance of the fluorescing molecule from the metallic film—ranging from quenching of fluorescence when the molecules are adjacent to the metal to predominantly free-space emission when the molecules are far from the metal. Within the distance range of coupling into the surface plasmon, the coupling strength is not uniform throughout, resulting in an optimum distance where the maximum intensity is emitted.

In our experiments, the SPCE fluorescence intensity is compared directly to the metal-free case. To accomplish this, slides were half-coated with silver and overlaid by a silica layer with desired thickness, and the dye was immobilized over the whole area by the method described earlier. A schematic of the sample configuration is shown in Fig. 7. The assumption of homogenous surface coverage density over the whole slide is crucial for ratiometric intensity evaluation. This assumption can be justified by the fact that the dye is immobilized onto a single type of surface, with no reason for variations across either type of material underneath. Moreover, ratiometric analysis ensures independence of the experimental geometry (distance from prism to detector, dimensions of prism, and illuminated spot diameter). Here, two samples were prepared for each thickness value. Two scans were performed on each of the metal and metal-free areas of the slide, the total intensity was calculated and averaged, and the ratio of intensity with metal (SPCE) and without metal was plotted.

The results of the SPCE:(metal-free) ratio measurements (triangles) are shown in Fig. 6 along with the previous metal-free intensity data (circles). The results indicate that the optimum silica spacer thickness for a single emission peak is 135 nm for our experimental conditions. It can be seen in Fig. 6 that the intensity corresponding to this spacer thickness is only $\sim 30\%$ of that measured in the absence of a metal layer. For more distant molecules, weaker coupling results in weaker fluorescence emitted into glass. By moving toward larger values of spacer thickness (when the condition for the existence of waveguide modes within the spacer layer is fulfilled) the total outcoupled intensity rises by a factor of two to 60% of the metal-free intensity, corresponding to a spacer thickness of ~ 340 nm. When the SAF component was extracted from the total emission, it was found that the SPCE/SAF ratio increases to $\sim 60\%$ in the lower spacer thickness region. This reduction in SPCE intensity compared to the metal-free case is consistent with theoretical work by Enderlein and Ruckstuhl,¹⁹ where the SPCE intensity was predicted to be attenuated irrespective of the mode of excitation (Kretschmann or reverse-Kretschmann) and the attenuation was predicted for both horizontal and vertical dipole orientation. Much of this attenuation is a result of absorption in the metal film, and it has been reported that the attenuation is strongest for the molecules very close to the metallic film as a

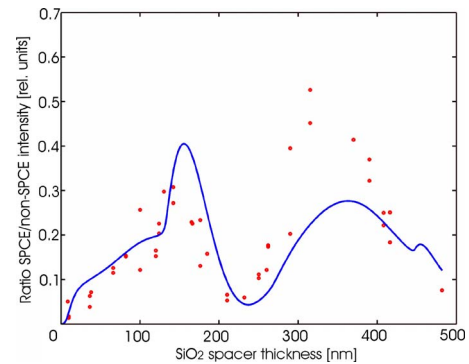


Fig. 8 Comparison of the experimental ratiometric data (dots) and the model curve (solid line).

consequence of a fast decoupling into the metal, accompanied by a significant reduction of fluorescence lifetime.^{19,28} A recent study¹³ using Langmuir-Blodgett films as spacer layers presented experimental and theoretical data that also confirmed the angular distribution behavior of SPCE.

In Fig. 8, the ratiometric experimental data that were plotted in the bottom half of Fig. 6 were compared with the theoretical model. The parameters of the model are exactly matched to the experimental parameters. Agreement between the experimental data (dots) and the model curve (solid line) is very good up to ~ 300 nm of silica thickness. However, for large values of SiO_2 thickness, although there is a general agreement with regard to the thickness value that yields maximum ratiometric signal, the experimental data for the second peak yields a maximum ratiometric signal that is about twice that of the theoretical value. The origin of this discrepancy is not yet clear and is under investigation by the authors.

5 Conclusions

In this work, we have studied the emission profile and dependence of emitted intensity on the metal-fluorophore spacer thickness for a silver-Cy5 dye SPCE system. The broad range of silica spacer layer thickness was chosen to facilitate a comparison between experimental results and the results of theoretical modeling.¹⁷⁻¹⁹ Excellent agreement was achieved between model and experiment for the ADE and its variation with spacer thickness. From the quantitative analysis of the metal-dye separation dependence, we demonstrate for the first time that SPCE intensity is reduced compared to the data obtained in the absence of the metal layer, as predicted in Ref. 19 and by the model used here. For single-peak SPCE emission, a maximum intensity of 30% of the metal-free value was achieved at the optimal metal-dye spacer thickness of 135 nm. Overall, good agreement was obtained between experimental results and the theoretical model.

Despite the complexity of the system and the decreased fluorescence intensities achievable with SPCE, we believe that because of its unique features of high directionality, surface sensitivity, and subsequent bulk fluorescence rejection capability, the technique has the potential for use in highly sensitive fluorescence-based biosensors. In this context, the data presented herein and the good agreement between theoretical model and experiment provide a strong basis for identifying the optimum design parameters for biosensor and bio-

assay platforms based on SPCE. The exploitation of these concepts will form the basis of future papers from us.

Acknowledgments

This material is based upon works supported by the Science Foundation Ireland under Grant No. 05/CE3/B754.

References

1. T. Hirschfeld, "Total reflection fluorescence," *Can Spectrosc.* **10**, 128 (1965).
2. D. Axelrod, T. P. Burghardt, and N. L. Thompson, "Total internal reflection fluorescence," *Annu. Rev. Biophys. Bioeng.* **13**, 247–268 (1984).
3. T. Ruckstuhl, J. Enderlein, S. Jung, and S. Seeger, "Forbidden light detection from single molecules," *Anal. Chem.* **72**(9), 2117–2123 (2000).
4. T. Ruckstuhl, M. Rankl, and S. Seeger, "Highly sensitive biosensing using a supercritical angle fluorescence (SAF) instrument," *Biosens. Bioelectron.* **18**(9), 1193–1199 (2003).
5. A. Krieg, S. Laib, T. Ruckstuhl, and S. Seeger, "Fast detection of single nucleotide polymorphisms (SNPs) by primer elongation using supercritical angle fluorescence," *ChemBioChem* **5**(12), 1680–1685 (2004).
6. T. Liebermann and W. Knoll, "Surface-plasmon field-enhanced fluorescence spectroscopy," *Colloids Surf., A* **171**, 115–130 (2000).
7. F. Yu, D. F. Yao, and W. Knoll, "Surface-plasmon field-enhanced fluorescence spectroscopy studies of the interaction of the interaction of an antibody and its surface-coupled antigen," *Anal. Chem.* **75**(11), 2610–2617 (2003).
8. G. Stengel and W. Knoll, "Surface plasmon field-enhanced fluorescence spectroscopy studies of primer extension reactions," *Nucleic Acids Res.* **33**(7), e69 (2005).
9. J. R. Lakowicz, "Radiative decay engineering 3. Surface plasmon-coupled directional emission," *Anal. Biochem.* **324**(2), 153–169 (2004).
10. I. Gryczynski, J. Malicka, Z. Gryczynski, and J. R. Lakowicz, "Radiative decay engineering 4. Experimental studies of surface plasmon-coupled directional emission," *Anal. Biochem.* **324**(2), 170–182 (2004).
11. E. Matveeva, Z. Gryczynski, I. Gryczynski, J. Malicka, and J. R. Lakowicz, "Myoglobin immunoassay utilizing directional surface plasmon-coupled emission," *Anal. Chem.* **76**(21), 6287–6292 (2004).
12. I. Gryczynski, J. Malicka, K. Nowaczyk, Z. Gryczynski, and J. R. Lakowicz, "Effects of sample thickness on the optical properties of surface plasmon-coupled emission," *J. Phys. Chem. B* **108**(32), 12073–12083 (2004).
13. K. Ray, H. Szmajcinski, J. Enderlein, and J. R. Lakowicz, "Distance dependence of surface plasmon-coupled emission observed using Langmuir-Blodgett films," *Appl. Phys. Lett.* **90**(25), 251116 (2007).
14. W. H. Weber and C. F. Eagen, "Energy-transfer from an excited dye molecule to the surface-plasmons of an adjacent metal," *Opt. Lett.* **4**(8), 236–238 (1979).
15. E. Matveeva, J. Malicka, I. Gryczynski, Z. Gryczynski, and J. R. Lakowicz, "Multi-wavelength immunoassays using surface plasmon-coupled emission," *Biophys. Biochem. Res. Comm.* **313**(3), 721–726 (2004).
16. F. D. Stefani, K. Vasilev, N. Bocchio, N. Stoyanova, and M. Kreiter, "Surface-plasmon-mediated single-molecule fluorescence through a thin metallic film," *Phys. Rev. Lett.* **94**(2), 023005 (2005).
17. N. Calander, "Theory and simulation of surface plasmon-coupled directional emission from fluorophores at planar structures," *Anal. Chem.* **76**(8), 2168–2173 (2004).
18. N. Calander, "Surface plasmon-coupled emission and Fabry-Perot resonance in the sample layer: a theoretical approach," *J. Phys. Chem. B* **109**(29), 13957–13963 (2005).
19. J. Enderlein and T. Ruckstuhl, "The efficiency of surface-plasmon-coupled emission for sensitive fluorescence detection," *Opt. Express* **13**(22), 8855–8865 (2005).
20. C. A. Goss, D. H. Harych, and M. Majda, "Application of (3-Mercaptopropyl)trimethoxysilane as a molecular adhesive in the fabrication of vapor-deposited gold electrodes on glass substrates," *Anal. Chem.* **83**(1), 85–88 (1991).
21. J. Kerimo, D. M. Adams, P. F. Barbara, D. M. Kaschak, and T. E. Mallouk, "NSOM investigations of the spectroscopy and morphology of self-assembled multilayered thin films," *J. Phys. Chem. B* **10**(47), 9451–9460 (1998).
22. J. D. Jackson, *Classical Electrodynamics*, Wiley & Sons, New York (1999).
23. J. Enderlein, T. Ruckstuhl, and S. Seeger, "Highly efficient optical detection of surface-generated fluorescence," *Appl. Opt.* **38**(4), 724–732 (1999).
24. J. Enderlein, "A theoretical investigation of single-molecule fluorescence detection on thin metallic layers," *Biophys. J.* **78**(4), 2151–2158 (2000).
25. J. Enderlein, "Single-molecule fluorescence near a metal layer," *Chem. Phys.* **247**(1), 1–9 (1999).
26. L. Polerecky, J. Hamrle, and B. D. MacCraith, "Theory of the radiation of dipoles placed within a multilayer system," *Appl. Opt.* **39**(22), 3968–3977 (2000).
27. G. Winter and W. L. Barnes, "Emission of light through thin silver films via near-field coupling to surface plasmon polaritons," *Appl. Phys. Lett.* **88**(5), 051109 (2006).
28. K. Vasilev, F. D. Stefani, V. Jacobsen, W. Knoll, and M. Kreiter, "Reduced photobleaching of chromophores close to a metal surface," *J. Chem. Phys.* **120**(14), 6701–6704 (2004).